PCCP

ROYAL SOCIETY OF CHEMISTRY

PERSPECTIVE

View Article Online
View Journal

Cite this: DOI: 10.1039/d6cp00187d

The melting properties of choline chloride in the representation of deep eutectic system phase diagrams

Ahmad Alhadid, [a] Mirjana Minceva, [b] João A. P. Coutinho [c] and Simão P. Pinho *[d]

Choline chloride (ChCl) is the cornerstone of deep eutectic solvents (DES), yet its melting properties remain an important source of uncertainty in the thermodynamic description of eutectic systems. Since ChCl decomposes before melting, reported values of its melting temperature (597 to 687 K) and enthalpy (4.3 and 13.8 kJ mol^{-1}) vary widely, while for the heat capacity change between solid and liquid states, only an estimate exists at 298.15 K. All these factors propagate inconsistencies into solid–liquid equilibrium (SLE) modelling, activity coefficient estimation, and data-driven approaches such as machine learning. In this work, we critically assess the melting properties of ChCl reported in the literature and evaluate their impact on the representation of phase diagrams of eutectic systems. By analysing the description of representative binary systems (ChCl + ionic compound, ChCl + water, and ChCl + urea), we demonstrate that neglecting the heat capacity change upon melting can lead to a substantial underestimation of the melting enthalpy. Thermodynamic modelling using NRTL-based approaches further reveals a strong interdependence between melting properties, liquid-phase nonideality, and the interpretation of experimental SLE data. Our results indicate that melting enthalpy values between 8 and 10 kJ mol^{-1}, combined with a non-negligible heat capacity change upon melting in the range 20–40 J mol^{-1} K^{-1}, provide the most consistent description across systems. This study clarifies the role of ChCl melting properties in the thermodynamic description of eutectic systems, providing a robust framework for enhancing the reliability of phase diagram interpretation, model development, and data-driven predictions in DES research.

Received 19th January 2026,
Accepted 31st March 2026

DOI: 10.1039/d6cp00187d

rsc.li/pccp

Introduction

Choline chloride (ChCl) is undoubtedly the most used substance in forming deep eutectic solvents (DESs). The term DES emerged around 2003 when Abbott and co-authors proposed using ChCl-based eutectic mixtures as novel solvents.[1] In their pioneering work, they introduced the concept of employing eutectic mixtures characterised by a significant depression of the melting temperature as novel designer solvents, with the ChCl + urea system serving as an example. Their work opened the door to the exploration of other systems and quickly expanded the field for applications in many areas of technology, including metal extraction, distillation or liquid–liquid extraction, biocatalysis, biomass processing, and the development of vehicles for the solubilization, transport, and bioavailability of active ingredients in the pharmaceutical industry, among others.[2,3]

In 2018, a proposal was made to establish a clear basis for the terminology related to DES, aiming to prevent ambiguities and ensure the use of scientifically accurate terms.[4] In that paper, the importance of measuring the solid–liquid equilibria (SLE) phase diagram of these mixtures was highlighted. It was also shown how significant it is to know the properties of DES constituents, such as melting temperature, melting enthalpy, and heat capacities at both liquid and solid phases, which are often not directly accessible through experiments using calorimetric techniques. This is the case with ChCl, which decomposes before melting. While a few "experimental" values of the melting temperature are available, varying from 575.15 to 588.75 K (sometimes reporting issues related to decomposition),[1,5,6] the first value for the melting

[a] College of Engineering and Technology, American University of the Middle East, Kuwait
[b] Biothermodynamics, TUM School of Life Sciences, Technical University of Munich, Freising, Germany
[c] CICECO – Aveiro Institute of Materials, Department of Chemistry, University of Aveiro, 3810-193 Aveiro, Portugal
[d] CIMO-Mountain Research Center, LA SusTEC, Bragança Polytechnic University, Campus of Santa Apolónia, Bragança, Portugal. E-mail: spinho@ipb.pt; Fax: +351 273 313 051; Tel: +351 273 303 086

enthalpy, estimated by an indirect method, was published in 2017.[7]

Accurate knowledge of the melting properties of DES constituents is essential to correctly evaluate the system thermodynamic behaviour and quantify deviations from ideality. Activity coefficients are key parameters in the thermodynamic modelling of DES, and inaccurate data can lead to both poor and seemingly good predictions, potentially resulting in misleading conclusions about a model's ability to describe SLE in DES. Furthermore, as machine learning (ML) becomes increasingly integrated into this field,[8,9] the importance of reliable melting properties and high-quality SLE data continues to grow. Melting properties are also critical for assessing the quality and consistency of published experimental datasets.[10]

As many DES are composed of ChCl, the work by Fernandez *et al.*[7] contributed to developing new perspectives in this field. Starting from the concepts of colligative properties, Pyykkö[11] proposed an empirical approach to estimate the eutectic point, while Kollau *et al.*[12] developed a strategy to assess the composition range of mixtures that remain in the liquid state at room temperature. On the other hand, Alhadid *et al.*[13] used a parametric study confirming the extreme importance of the melting properties of the DES constituents in understanding and designing new DES systems. The authors showed that due to the interrelation between the melting properties and the activity coefficients of the DES components, the SLE phase diagrams of a DES can be effectively described by adjusting different melting enthalpy values. Lower melting enthalpies resulted in behavior that closely approximates an ideal liquid phase,

Ahmad Alhadid

Dr Ahmad Alhadid is an Assistant Professor of Chemical Engineering at the College of Engineering and Technology, American University of Middle East (AUM), Kuwait. He holds a PhD from the Technical University of Munich, awarded summa cum laude (highest distinction). His research focuses on advancing sustainable and environmentally conscious technologies through expertise in green solvent design, chemical thermodynamics, and innovative processing methods.

Mirjana Minceva

Dr Mirjana Minceva holds a professorship in Biothermodynamics at the Technical University of Munich. She completed her PhD in chemical engineering at the University of Porto, Portugal and her habilitation in separation processes at the Friedrich-Alexander-University Erlangen-Nuremberg, German. Her main field of research is the application of thermodynamics to develop efficient separation processes in the downstream processing of biomolecules. The research methodology involves model-based process design with the approach "from molecule to process" and bridges the gap between understanding molecular-level phenomena and process implementation.

João A. P. Coutinho

João A. P. Coutinho is a Full Professor at the Chemistry Department of University of Aveiro, Portugal, where he is the director of CICECO, one of the leading European Laboratories in Materials Science. He leads a multidisciplinary research team that focuses on the development of green solvents and novel separation processes for use in biorefinery and circular economy systems. Currently he strives to apply biobased solvents, DES and ionic liquids to these processes and attempts to better understand their physical–chemical behavior.

Simão P. Pinho

Simão P. Pinho completed his PhD in Chemical Engineering at the University of Porto. He currently holds the position of Associate Professor (with Habilitation from Aveiro University) at Bragança Polytechnic Institute, where he is a permanent member of the Associate Laboratory SusTEC and the Mountain Research Center. His research focuses on biomolecules, electrolytes, eutectic solvents, and ionic liquids, with contributions from experimental methods to thermodynamic modeling, on physical properties and phase equilibria, bridging knowledge transfer within engineering and applied chemistry fields, while fostering a vision grounded in sustainability.

whereas higher values require the inclusion of activity coefficients to compensate for the high melting enthalpies and appropriately describe the SLE.

Applying the COSMO-RS model, Song *et al.*[14] showed that the accuracy of the model to represent SLE in eutectic systems depends heavily on the salt conformer choice, yielding reasonable eutectic temperature predictions but less accurate eutectic composition estimates, while Peng *et al.*[15] reported the inability to accurately predict SLE in salt-based eutectic systems, whether the salt was modeled as an ion pair or fully dissociated. This inaccuracy stems from both limitations in the model and unreliable melting data for thermally unstable salts.

Different methods for modelling phase equilibria and properties of deep eutectic solvents DES, including excess Gibbs energy (G^E) models, equations of state (EoS), and molecular dynamics (MD) simulations, have been applied.[16] Some G^E models and EoS approaches often treat DES as pseudo-components to simplify parameterization and calculations, limiting their applicability, while the use of group-contribution models such as UNIFAC[17–19] makes the approach more general, increasing the parameter transferability to other systems. More recently, a line of work combining thermodynamics and ML has been receiving significant attention. Specifically for predicting SLE phase diagrams and eutectic coordinates in systems containing salts such as ChCl, the melting temperature and enthalpy of the pure components are again important molecular descriptors.[20] However, the experimental difficulties associated with their determination, particularly for alkylammonium-based halides, make it very difficult to compute the melting point of DES accurately, as shown by Ayres *et al.*,[21] where all the melting point prediction outliers are from mixtures containing compounds such as ChCl. As the ML models for eutectic coordinates depend heavily on the melting properties of DES constituents and activity coefficients,[22] further efforts are necessary for the accurate systematization of the SLE experimental data, as reported in a review by López-Flores *et al.*[23] These experimental difficulties for measuring the SLE phase diagrams together with the melting property uncertainties of the pure ChCl leads to very different conclusions in terms of the eutectic coordinates, as recently discussed for an ethylene glycol + ChCl mixture.[24] For ChCl in particular, the published melting temperatures vary from 575.15 K to 687 K,[1,24] while the melting enthalpy is in the range 4.3–13.8 kJ mol^{-1}.[7,24] To the best of our knowledge, only an estimate for the heat capacity upon melting is available at 298.15 K, which is 39.3 J mol^{-1} K^{-1}.[25]

In this context, this paper critically reviews and discusses the various melting properties of ChCl reported in the open literature. It presents a detailed evaluation of data, comparing and testing different published values and their impact on the representation of binary phase diagrams of ChCl with ionic compounds, water, or urea, firstly considering the ideality of the liquid phase. In a complementary perspective, this systematic investigation is further deepened using NRTL-based approaches to model different thermodynamic properties and SLE of the systems ChCl + water and ChCl + urea, analyzing the influence of ChCl melting properties on the phase diagram representations and liquid phase nonideality quantification, performing a sensitivity analysis.

ChCl melting properties

ChCl exhibits several notable structural characteristics. It is a quaternary ammonium salt composed of a bulky choline cation and a small chloride anion, resulting in significant charge asymmetry. The chloride ion has a high charge density, whereas the choline cation features a positively charged nitrogen center and a hydroxyl group capable of hydrogen bonding. This combination imparts dual characteristics: high polarity and the capacity for both strong ionic and hydrogen-bonding interactions, occurring intra- and intermolecularly. These interactions explain ChCl's well-defined solid–solid phase transition and relatively high melting temperature compared to many organic compounds, although it seems to melt at a lower temperature than typical inorganic salts. Additionally, this structural makeup accounts for its pronounced hygroscopic nature. While the solid–solid transition between α and β phases is well-defined, reversible, and associated with high enthalpy and entropy changes,[25] the melting is not well-defined. Besides the plastic crystalline character of the β phase,[26] the tendency to undergo irreversible changes, decomposition at high temperatures, and its strong hygroscopic nature complicates both the experimental handling and the interpretation of phase behavior data.

Short historical perspective

For eutectic systems with complete immiscibility in the solid phase, a solid–solid transition, and a constant heat capacity change upon melting, the solid–liquid equilibrium can be described by:[27]

$$\begin{aligned}\ln x_i\gamma_i = &\frac{\Delta H_{m,i}}{RT}\left(\frac{T}{T_{m,i}}-1\right)+\frac{\Delta H_{tr,i}}{RT}\left(\frac{T}{T_{tr,i}}-1\right)\\ &-\frac{\Delta C_{p,m,i}}{R}\left(1-\frac{T_{m,i}}{T}+\ln\frac{T_{m,i}}{T}\right)\\ &-\frac{\Delta C_{p,tr,i}}{R}\left(1-\frac{T_{tr,i}}{T}+\ln\frac{T_{tr,i}}{T}\right)\end{aligned} \quad (1)$$

where x_i is the mole fraction solubility of compound i and γ_i its activity coefficient in the liquid phase, $\Delta H_{m,i}$ and $T_{m,i}$ are the molar melting enthalpy and temperature, $\Delta H_{tr,i}$ and $T_{tr,i}$ are the solid–solid molar transition enthalpy and temperature, R is the ideal gas constant, T is the absolute temperature, and $\Delta C_{p,m,i}$ is the difference between the molar heat capacity of the compound i in liquid and solid phases, while $\Delta C_{p,tr,i}$ is its equivalent for the solid–solid transition.

If considering only data above the solid–solid transition temperature, neglecting the term related to the heat capacity

change upon melting and assuming the liquid phase as an ideal mixture, eqn (1) becomes:

$$\ln x_i = \frac{\Delta H_{m,i}}{RT_{m,i}} + \frac{\Delta H_{m,i}}{RT} \quad (2)$$

Eqn (2) served as the basis for the first estimation of the melting enthalpy of ChCl by Fernandez *et al.*,[7] through the fitting of experimental SLE data. A large set of ionic systems was initially studied, from which ten were identified as forming ideal liquid solutions. Thermodynamic consistency tests recently proposed by NIST[28] and DTU[29] were applied to validate the experimental data. The systems that were considered ideal were selected based on the ChCl mole fraction ratios, at the same temperature, in two different binary systems, which are equivalent to activity coefficient ratios. These ratios ranged from 0.93 to 1.07, guaranteeing at least similar deviations from the ideal solution, further confirmed by calculating the activity coefficients by COSMO-RS.

Based on the assumptions of eqn (2) and using the SLE data of the ten selected systems, always above the solid–solid transition temperature (351 ± 3 K),[30] the estimated melting temperature and enthalpy were 597 ± 7 K and 4.3 ± 0.6 kJ mol^{-1}, respectively. When applying a similar linear fit to the SLE data of each of the ten systems individually, the corresponding values fell within the range 589–632 K for the melting temperature and 3.7–5.5 kJ mol^{-1} for the melting enthalpy.

Considering the value of solid–solid transition enthalpy (16.5 ± 0.2 kJ mol^{-1})[30] at 351 K, the estimated melting enthalpy of 4.3 ± 0.6 kJ mol^{-1} is remarkably low. Consequently, a comprehensive study to measure the solubility of ten alkylammonium halide salts (chlorides and bromides) in water was started.[31] Using density and water activity data of these binary mixtures, parameters for a PC-SAFT-based model were initially estimated. Using the PC-SAFT model to calculate the salt activity coefficients and combining them with experimental solubility data, the melting enthalpies of the salts were estimated, assuming a melting temperature of 597 K and neglecting heat capacity contributions. For ChCl, the estimated melting enthalpy for a melting temperature of 597 K was 7.8 kJ mol^{-1}.[31]

In 2023, using ultra-fast scanning calorimetry in combination with micro X-ray diffraction and high-speed optical microscopy, van den Bruinhorst *et al.*[24] measured the melting temperature and enthalpy of ChCl, reporting values of 687 ± 9 K and 13.8 ± 3.0 kJ mol^{-1}, respectively. These data differ significantly from previously estimated values, highlighting the need for further studies. An initial contribution in this direction was made by Correa *et al.*,[32] who simulated the phase transition of ChCl using different atomistic force fields through molecular dynamics. Although the limited availability of experimental data for the liquid phase of ChCl and the high sensitivity to the choice of force field constrain the accuracy of these computational approaches, their study suggests a melting temperature of 627 K and a melting enthalpy of 7.8 kJ mol^{-1}. Table 1 summarizes the published values of the melting properties of ChCl.

Heat capacity impact

Because changes in heat capacity upon melting are often unknown, they are typically neglected in calculations. While this omission usually has only a minor effect on solubility estimates, it can become significant when the enthalpy of melting is small, and there is a large temperature difference between the mixture's melting point and that of the pure compound. That is the case with most of the SLE phase diagrams of binary mixtures containing ChCl. For this reason, eqn (2) should more correctly maintain the heat capacity term and be written as:

$$\ln x_i = \frac{\Delta H_{m,i}}{RT}\left(\frac{T}{T_{m,i}} - 1\right) - \frac{\Delta C_{p,m,i}}{R}\left(1 - \frac{T_{m,i}}{T} + \ln\frac{T_{m,i}}{T}\right) \quad (3)$$

Fig. 1 illustrates the average weight percentage, defined as the ratio of the heat capacity term value to the total value of the right-hand side of eqn (3), which encompasses both enthalpy and heat capacity terms contributions. This weight is calculated as an average in the temperature interval from the solid–solid transition temperature (351 K) and the fixed melting temperature of ChCl (600 or 700 K). This temperature range was selected to match the temperature interval of the experimental data of the binary ionic systems initially used to estimate the ChCl melting properties *via* eqn (2). Due to the uncertainty of the melting properties of ChCl (see Table 1), the calculations were carried out at two melting temperatures (600 and 700 K) and three different melting enthalpies (4, 8 and 14 kJ mol^{-1}) within the range of published melting properties, varying the heat capacity change from 0 to 50 J mol^{-1} K^{-1}. As expected, the contribution of the heat capacity term increases with the decrease in melting enthalpy and the increase in melting temperature. In the context of this work, it is important to highlight that at the lowest melting enthalpy (4 kJ mol^{-1}), the heat capacity term shows an average weight percentage higher than 25% for $\Delta C_{p,m}$ = 20 J mol^{-1} K^{-1} and increases to 40% for $\Delta C_{p,m}$ = 40 J mol^{-1} K^{-1}, which is a very likely the $\Delta C_{p,m}$ value.

Table 1 Compilation of the melting temperature and enthalpy of choline chloride, methods and sources

T_m/K	ΔH_m/kJ mol^{-1}	Method	Ref.
597 ± 7	4.3 ± 0.6	ChCl solubility in binary ideal systems	Fernandez *et al.*[7]
597	7.8	ChCl solubility in water + PC-SAFT	Vilas-Boas *et al.*[31]
687 ± 9	13.8 ± 3.0	Fast-DSC on pure ChCl	Bruinhorst *et al.*[24]
627	7.8	Molecular dynamics of pure ChCl	Correa *et al.*[32]

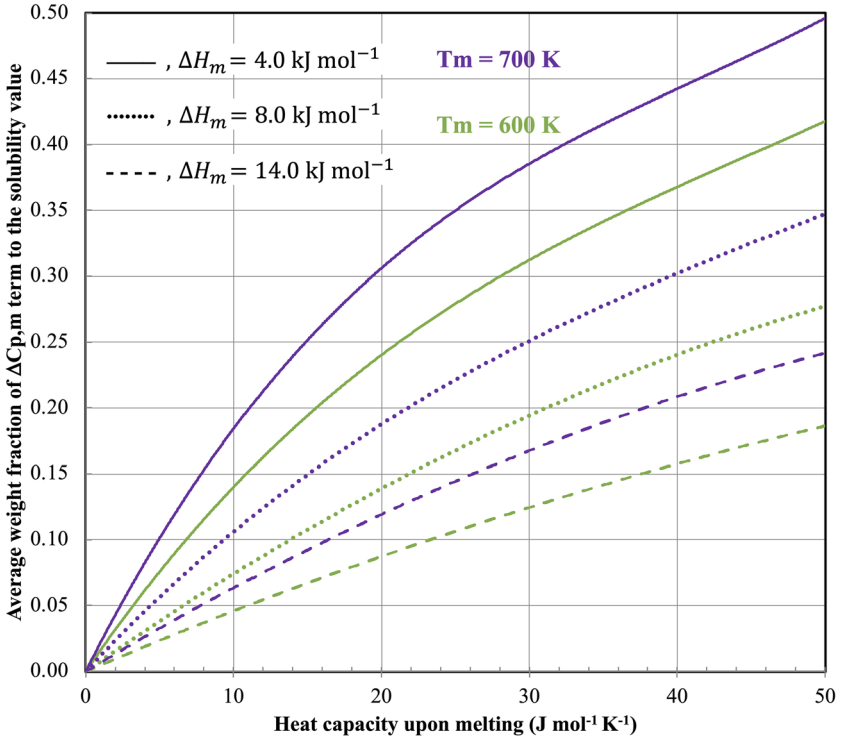

Fig. 1 Average weight percentage of the heat capacity term in the SLE eqn (1) for choline chloride, depending on the heat capacity change upon melting, at different melting temperatures.

At this same $\Delta C_{p,m}$ value, even at a melting enthalpy of 14 kJ mol^{-1}, the average weight percentage is as high as 20%.

For the lowest value of the melting enthalpy (4 kJ mol^{-1}) in Fig. 1, neglecting the heat capacity term can be a critical simplification. Given that the first reported[7] ChCl melting enthalpy is 4.3 kJ mol^{-1}, which was estimated by neglecting the heat capacity term, it is essential to explore how neglecting that term may have influenced the estimated value for the ChCl enthalpy of melting. Considering the ideality of the liquid phase again and using eqn (3), hypothetical solubility lines for ChCl were calculated between the solid–solid transition temperature and a fixed melting temperature (600 or 700 K), across a range of heat capacities (0–50 J mol^{-1} K^{-1}) and melting enthalpies (0–40 kJ mol^{-1}). These hypothetical solubility values were obtained by linearizing eqn (2), and new melting enthalpy and temperature values were estimated, neglecting, for comparison purposes, the heat capacity term.

Fig. 2 illustrates the decrease in the calculated melting enthalpy at two different melting temperatures, compared to the fixed melting enthalpy value used in eqn (2). This is the

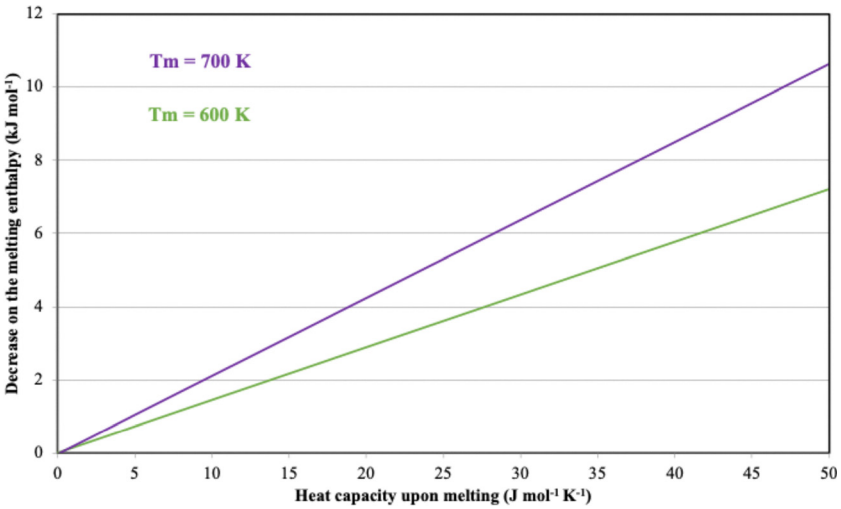

Fig. 2 Melting enthalpy increment to be added to the melting enthalpy estimated from eqn (2), neglecting the heat capacity term.

most significant result of this analysis, as the estimated enthalpy of melting is consistently higher than the fixed value, and this increment grows linearly with the heat capacity change (Fig. 2). To better understand the relevance of Fig. 2, consider the following example for clarification. When $\Delta C_{p,m}$ = 30 J mol^{-1} K^{-1} and T_m = 600 K, the enthalpy of melting neglecting the $\Delta C_{p,m}$ term is underestimated by approximately 4 kJ mol^{-1}. Consequently, with an estimated temperature of 597 K[7] and considering $\Delta C_{p,m}$ = 30 J mol^{-1} K^{-1}, the real enthalpy would be 8.3 kJ mol^{-1} (4 kJ mol^{-1} above the first melting enthalpy value estimated by Fernandez *et al.*[7]). A similar underestimation of 4 kJ mol^{-1} is observed when $\Delta C_{p,m}$ = 20 J mol^{-1} K^{-1} but T_m = 700 K. The magnitude of this underestimation does not depend on the fixed value of the melting enthalpy, but only on the assumed value of the heat capacity change. With respect to the melting temperatures, the re-estimated values are always slightly higher than the original values, more for lower melting enthalpies and higher $\Delta C_{p,m}$ values.

Melting properties in the description of ideal SLE phase diagrams

Ionic binary systems

Initially, the different sets of melting properties compiled in Table 1 were used in eqn (3) to calculate the ideal ChCl solubility line and compare it with the experimental data measured for binary salt mixtures containing ChCl.[7] Fig. 3(a) presents such a comparison, when neglecting the $\Delta C_{p,m}$ term (eqn (2)). Unsurprisingly, the best agreement was obtained using the values proposed by Fernandez *et al.*[7] In contrast, when employing melting properties measured by fast-DSC,[24] the deviations from the experimental data become notably significant.

In Fig. 3(b), the predictions are carried out using eqn (3), with the value of $\Delta C_{p,m}$ fixed at 30 J mol^{-1} K^{-1}. It is evident that the melting temperature and enthalpy reported by Fernandez *et al.*,[7] when combined with this $\Delta C_{p,m}$ value, yield a representation of the liquidus line that lacks physical meaning. The calculated solubility line would also suggest strong positive deviations from ideality in these systems, which is not expected. On the other hand, the melting properties reported by van den Bruinhorst *et al.*[24] would indicate a significant negative deviation from ideality, even at ChCl mole fractions approaching one. This behavior is also not physically plausible since activity coefficients should tend toward unity under these conditions. Overall, the intermediate melting properties reported by Vilas-Boas *et al.*[31] and Correa *et al.*[32] provide a more consistent description of the experimental data when $\Delta C_{p,m}$ of 30 J mol^{-1} K^{-1} is considered.

ChCl + neutral molecule systems

To evaluate the melting properties of ChCl on the description of other systems, the SLE phase diagrams of the binary ChCl + water and ChCl + urea systems were selected, given the amount and quality of data provided by various authors. Taking into account the range for the melting temperature and enthalpy reported in Table 1, and by selecting $\Delta C_{p,m}$ values ranging from 0 to 40 J mol^{-1} K^{-1}, the phase diagrams were calculated by eqn (1), under the assumption of ideal behavior in the liquid phase and taking into account the ChCl solid–solid transition. All other properties needed for these calculations are well-established, such as the melting properties of water (ΔH_m = 6.01 kJ mol^{-1} and T_m = 273.2 K), urea (ΔH_m = 14.6 kJ mol^{-1}, T_m = 407.2 K), and for the ChCl the solid–solid (ss) transition properties (T_{ss} = 352.2 K, ΔH_{ss} = 16.3 kJ mol^{-1} and $\Delta C_{p,ss}$ = 16 J mol^{-1} K^{-1}).[25]

ChCl + water system

Although in the DES study the COSMO-RS model showed limited accuracy in capturing the temperature effect on the activity coefficients, at 298.15 K, it provided a reliable approximation for the activity coefficients of water in the presence of

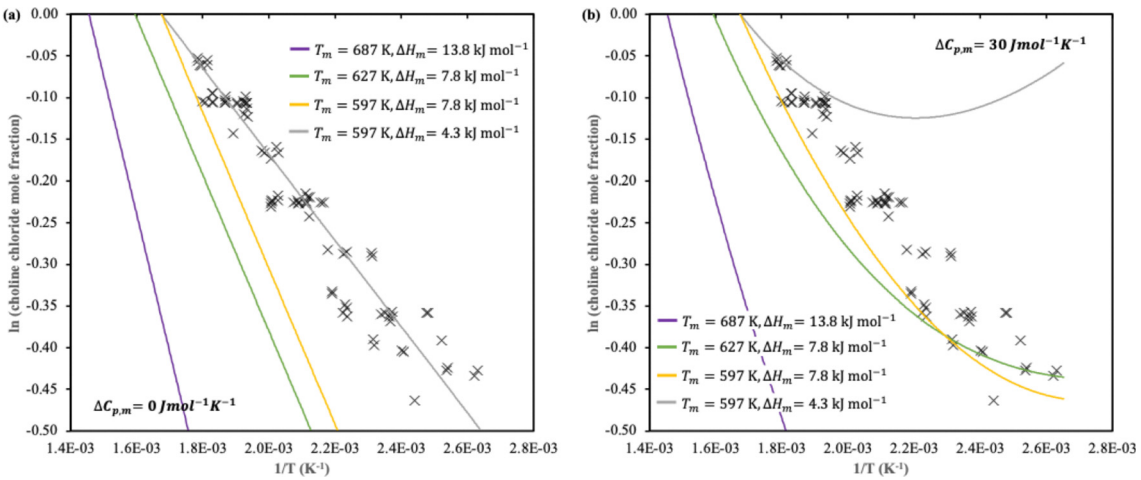

Fig. 3 Representation of ln x_{ChCl} as a function of 1/T: (a) $\Delta C_{p,m}$ = 0 J mol^{-1} K^{-1}, and (b) $\Delta C_{p,m}$ = 30 J mol^{-1} K^{-1}, using the different melting properties compiled in Table 1: Fernandez *et al.*;[7] Vilas-Boas *et al.*;[31] Bruinhorst *et al.*[24] and Correa *et al.*[32] The data points are from binary systems constituted by [Ch]Cl and [Ch][Ac], [Ch][Prop], [Ch][Buta], [N_{4444}]Cl, [P_{4444}]Cl, [BzCh]Cl, [C_4mpyr]Cl, [Ch][NTf_2], [C_2mim]Cl or [C_2OHmim]Cl.[7]

ChCl, derived from water activity measurements, indicating, at the same time, that the activity coefficient of ChCl is close to unity for ChCl mole fractions above 0.5.[25] Encouraged by this near-ideal behavior of ChCl, predictions of SLE phase diagrams by varying ChCl melting properties were compared against the experimental data to assess their reliability.

First, the melting temperature and enthalpy from Table 1 are used to explore the impact of introducing the $\Delta C_{p,m}$ term. When the change in heat capacity upon melting is neglected (Fig. 4a), none of the available data sets adequately represent the solubility line of ChCl. The data reported by Fernandez *et al.*[7] yield an unexpected positive deviation at higher temperatures, and a negative deviation below the solid–solid transition temperature. With $\Delta C_{p,m}$ = 20 J mol^{-1} K^{-1} (Fig. 4b) the magnitude of the negative deviation from ideality is significantly reduced. For the intermediate enthalpy value,[31,32] a small positive deviation from ideality at temperatures above the solid–solid transition temperature, and a physically implausible liquidus line are obtained when using the melting properties data from Fernandez *et al.*[7] This inconsistency becomes more pronounced with $\Delta C_{p,m}$ = 40 J mol^{-1} K^{-1} (Fig. 4c), where only the data from van den Bruinhorst *et al.*[24] yield a plausible representation of the solubility line. In all cases, increasing $\Delta C_{p,m}$ shifts the eutectic composition toward higher ChCl concentrations, and the evident discrepancy of the eutectic temperature to the experimental value becomes lower, but grows with increasing values of the melting properties.

Fig. 5 examines the influence of the melting enthalpy on the solubility lines of ChCl, using two different values of $\Delta C_{p,m}$ (Fig. 5a, c and e, $\Delta C_{p,m}$ = 15 J mol^{-1} K^{-1}, and Fig. 5b, d, and f, $\Delta C_{p,m}$ = 30 J mol^{-1} K^{-1}) across the reported melting temperature range. Within an amplitude of 90 K (range of the reported melting temperature from 597 to 687 K), the solubility lines exhibit minimal variation, provided all other melting properties remain constant. However, when higher melting temperatures are paired with the lowest melting enthalpy,[7] the resulting solubility lines become defective. These lines display significant positive deviations from ideality and, as previously noted, show growing physical inconsistencies with increasing values of $\Delta C_{p,m}$.

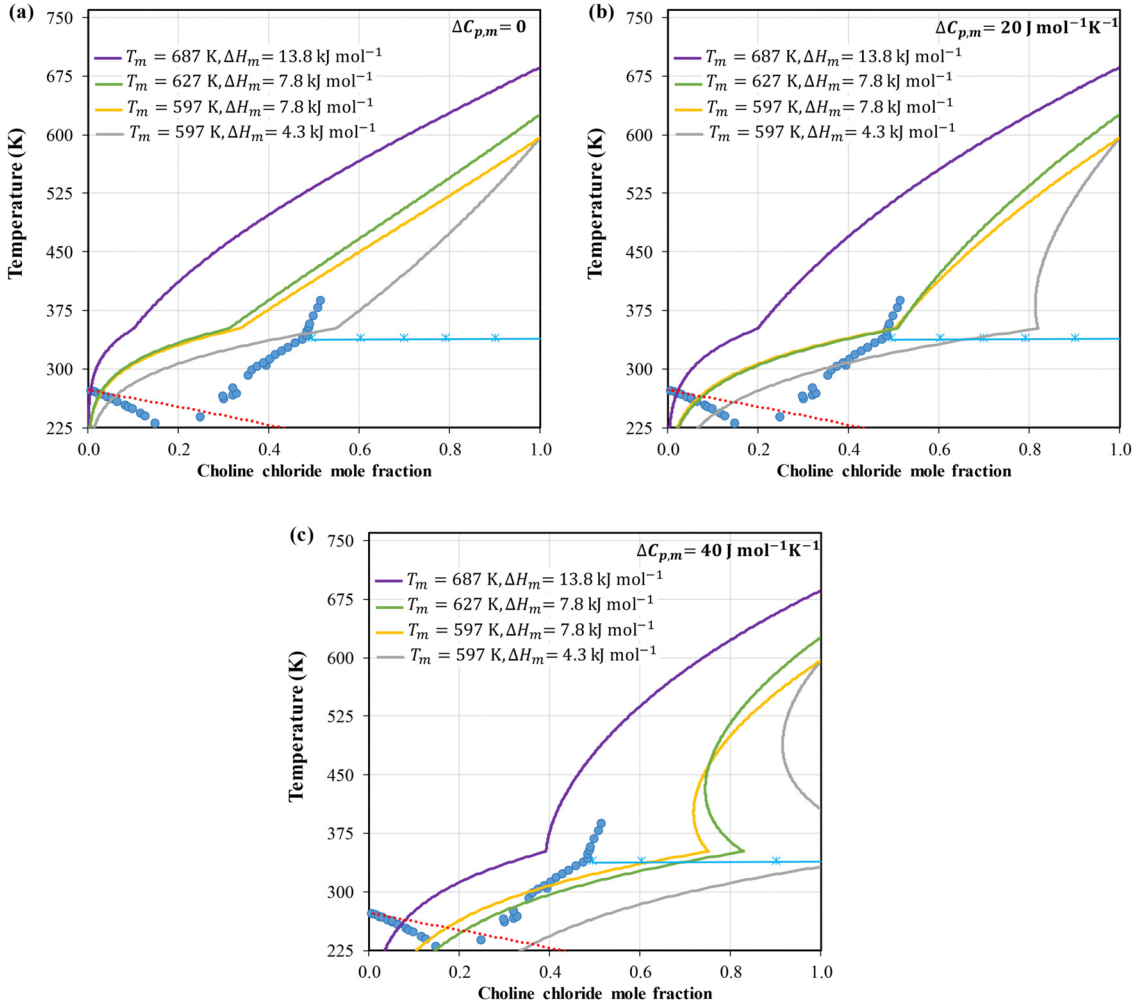

Fig. 4 Solid–liquid phase diagram for the ChCl + water system: (a) $\Delta C_{p,m}$ = 0 J mol^{-1} K^{-1}, (b) $\Delta C_{p,m}$ = 20 J mol^{-1} K^{-1}, and (c) $\Delta C_{p,m}$ = 40 J mol^{-1} K^{-1}, using the different melting properties compiled in Table 1: Fernandez *et al.*;[7] Vilas-Boas *et al.*;[31] Bruinhorst *et al.*[24] and Correa *et al.*[32] water solubility line, and solid–solid transition. ● and ✳ are data points from Lobo *et al.*[25]

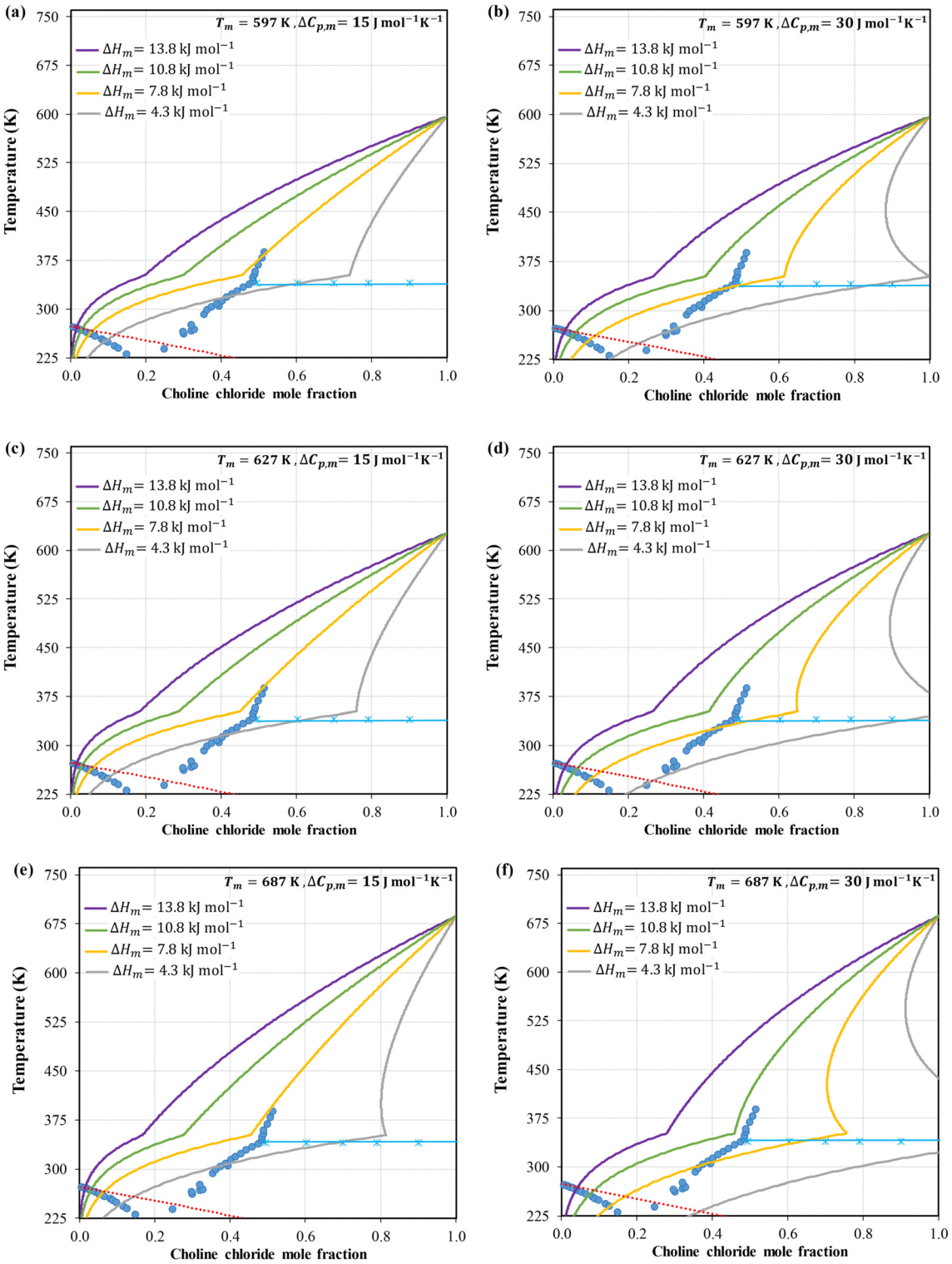

Fig. 5 Solid–liquid phase diagram for the ChCl + water system: (a) and (b) assuming the melting temperature reported by Fernandez *et al.*,[7] (c) and (d) assuming the melting temperature reported by Correa *et al.*,[32] and (e) and (f) assuming the melting temperature reported by van den Bruinhorst *et al.*[24] for different melting enthalpies: ——— ΔH_m = 4.3 kJ mol^{-1}; ——— ΔH_m = 7.8 kJ mol^{-1}; ——— ΔH_m = 10.8 kJ mol^{-1} and ——— ΔH_m = 13.8 kJ mol^{-1}. ····· water solubility line, and ——— solid–solid transition. ● and ✳ are data points from Lobo *et al.*[25]

It is important to highlight that as the melting enthalpy increases, the system exhibits a more pronounced negative deviation from ideality. This leads to a shift in the eutectic point towards lower ChCl mole fractions ($x_{E,ChCl}$) and significantly higher eutectic temperatures (T_E) compared to experimental observations ($x_{E,ChCl}$ = 0.20 and T_E = 204 K).[25] Notably, the experimental

solubility data above the solid–solid transition point are closer to the ChCl solubility line within the range of the melting enthalpies between 7.8 and 10.8 kJ mol^{-1}, as shown in Fig. 5.

ChCl + urea system

The same procedure was applied to the ChCl + urea system (Fig. 6). It was observed that, depending on the values of the melting enthalpy and temperature, there is a threshold value of $\Delta C_{p,m}$ beyond which the phase diagram yields unrealistic representations. Since the melting temperature has a relatively minor influence on the overall phase diagram, representations are displayed at 597 K and 687 K using two different $\Delta C_{p,m}$ values. For a ChCl melting temperature of 597 K, the most suitable melting enthalpy to represent the SLE phase diagram lies between 7.8 and 10.8 kJ mol^{-1}.

In contrast to the ChCl + water system, where the highest experimentally reported mole fraction of ChCl was 0.515, for the ChCl + urea system, data points are available until a composition of x_{ChCl} = 0.898. At this composition, the solubility line is not expected to deviate significantly from the ideal solution solubility line. This is observed when using a melting temperature of 597 K and an enthalpy of fusion of 7.8 kJ mol^{-1}, consistent across both used values of $\Delta C_{p,m}$. Despite the high uncertainty in the experimental data, often attributed to residual water in the mixture or degradation due to temperature effects, the most appropriate range of the melting enthalpy to model the SLE phase diagram appears to be between 7.8 and 10.8 kJ mol^{-1} when the melting temperature is 687 K. However, such a high melting temperature would present substantial negative deviations from ideality, particularly at high ChCl mole fractions, which is not expected. These deviations become even more pronounced when an enthalpy of fusion of 13.8 kJ mol^{-1} is used.

Non-ideal phase diagrams

The previous analysis assumes the ideal solution behavior, which provides hints for the most probable range of melting

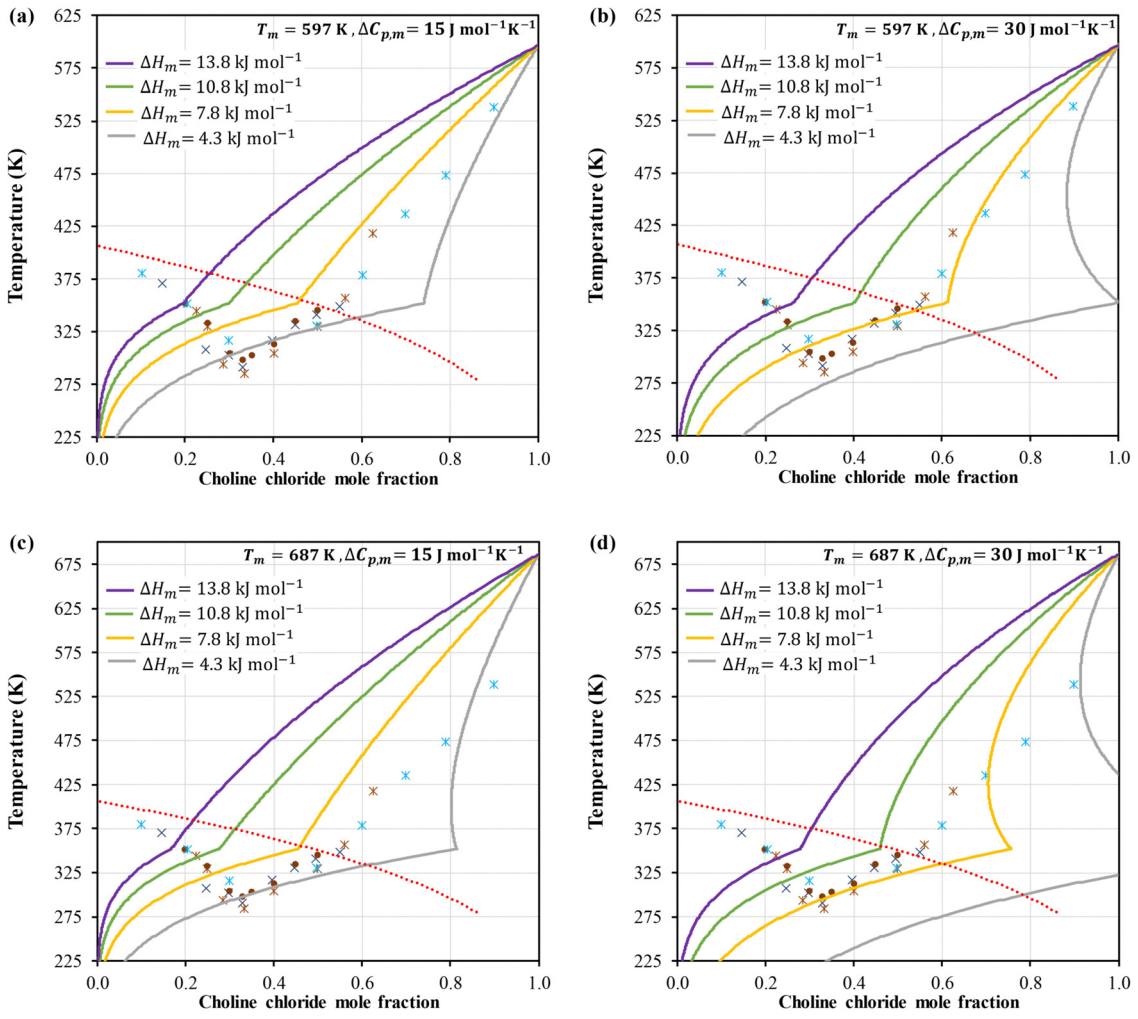

Fig. 6 Solid–liquid phase diagram for the ChCl + urea system: (a) and (b) assuming the melting temperature reported by Fernandez *et al.*[7] and (c) and (d) assuming the melting temperature reported by van den Bruinhorst *et al.*[24] at different melting enthalpies: —— ΔH_m = 4.3 kJ mol^{-1}; —— ΔH_m = 7.8 kJ mol^{-1}; —— ΔH_m = 10.8 kJ mol^{-1} and —— ΔH_m = 13.8 kJ mol^{-1}. ····· urea solubility line. Experimental data were taken from: × Abbot *et al.*[1] ✳ Morrison *et al.*[33] ● Meng *et al.*[34] and ✳ Silva *et al.*[35]

properties of ChCl and helps to understand the impact of the melting enthalpy, heat capacity change, and melting temperature on the calculated phase diagram. Nevertheless, for an accurate representation of the ChCl + water and ChCl + urea SLE phase diagrams, the solution nonideality must be taken into account. For ChCl + urea, ChCl was assumed as a neutral ion pair. On the other hand, two approaches based on the NRTL model were implemented to estimate the activity coefficients of components in the liquid phase for ChCl + water: (1) modelling ChCl as a neutral ion pair or (2) modelling ChCl as fully dissociated ions, adding in this case a Pitzer–Debye–Hückel long-range term. Recent work by Marques *et al.*[36] reported that considering the long-range ionic interactions improves the modelling of IL solutions.

For the ChCl + water system, different types of data sets are available in the literature, namely, vapor-liquid equilibrium (VLE),[37–39] water activity,[40,41] heat of mixing,[42] and mean ionic activity coefficient of ChCl from isopiestic measurements,[43–45] which were used to estimate the NRTL binary parameters. Due to the observed interrelation between the melting properties and the solution nonideality, the experimental SLE data for the ChCl + water system were not used for parameter estimation. Details on the modelling approaches and the estimation of binary parameters are provided in the supplementary information (SI). The NRTL binary parameters for ChCl + water are presented in Table S1 of the SI.

In contrast, only SLE data are available for the ChCl + urea mixture. Consequently, the melting enthalpy of ChCl and the NRTL binary parameters for the ChCl + urea system were determined by fitting to SLE data for both the ChCl + urea and ChCl + water systems. In this procedure, the NRTL binary parameters for ChCl + water were fixed to values previously estimated from non-SLE experimental data. The NRTL binary parameters for ChCl + urea and the estimated melting enthalpy values of ChCl can be found in Tables S2 and S3 in the SI, respectively. The urea activity calculated at the eutectic composition (urea mole fraction of 0.67) at various temperatures is of the correct order of magnitude compared to experimental data (see Fig. S2 in the SI),[46] confirming the reliability of the estimated binary parameters for ChCl + urea. The root-mean-square deviation between experimental and calculated data can be found in Table S4 in the SI.

Fig. 7a shows the melting enthalpy of ChCl estimated in this work, assuming the different melting temperatures reported for ChCl (Table 1) and the heat capacity change upon melting for ChCl. As shown in Fig. 7a, the ion pair (dashed line) and dissociated ion (solid lines) representations of ChCl yield very similar melting enthalpies. The melting enthalpy increases as $\Delta C_{p,m}$ increases. On the other hand, the melting temperature only slightly influences the values of ChCl melting enthalpy. In general, the estimated melting enthalpy at $\Delta C_{p,m}$ = 15 J mol^{-1} K^{-1} (blue lines) is in good agreement with those reported by Vilas-Boas *et al.*[31] (orange cross) and Correa *et al.*,[32] (yellow cross) at T_m = 597 and 627 K, respectively. On the other hand, the estimated melting enthalpy at $\Delta C_{p,m}$ = 30 J mol^{-1} K^{-1} (purple line) and T_m = 687 K is slightly lower than that found experimentally by van den Bruinhost *et al.*[24] (blue cross). Moreover, the estimated melting enthalpy at $\Delta C_{p,m}$ = 0 (grey line) and T_m = 597 K is slightly higher than that reported by Fernandez *et al.*[7] (green cross). As can be observed in Fig. 7b, the calculated melting entropy indicates that the estimated melting enthalpies fulfil Timmerman's criterion for the melting entropy of plastic crystalline materials $\left(i.e., \frac{\Delta S_m}{R} \leq 2\right)$.[47]

Although the estimated melting enthalpies are similar when assuming different modelling approaches or ChCl heat capacity change, the activity coefficients of ChCl in ChCl + water are different when regarding ChCl as ion pairs or dissociated ions

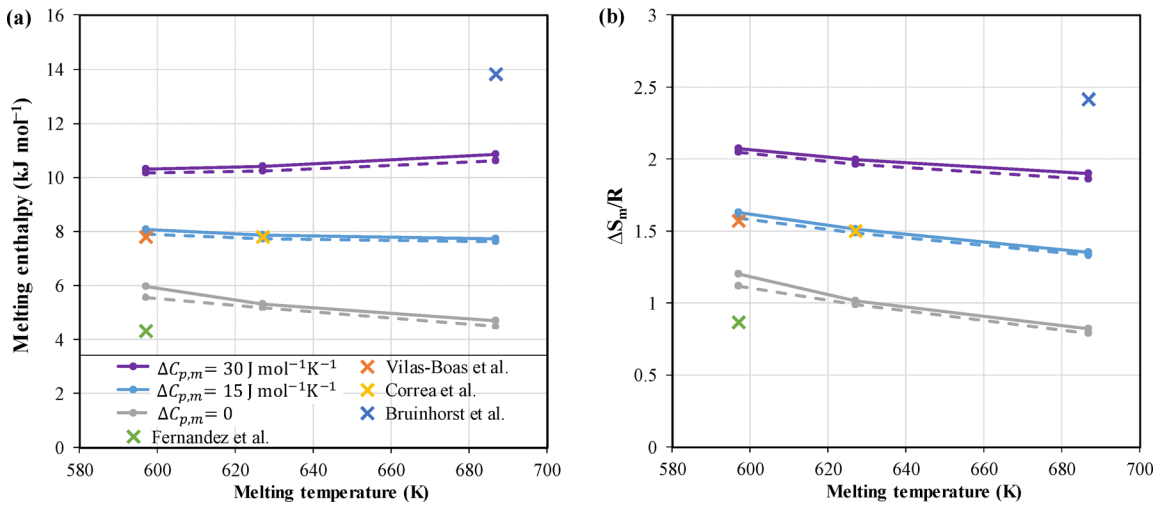

Fig. 7 The melting enthalpy (a) and entropy (b) of choline chloride (ChCl) estimated in this work, assuming different melting temperatures and heat capacity change of ChCl. Solid lines are data calculated when regarding ChCl as dissociated ions, and dashed lines are data calculated when considering ChCl as ion pairs in ChCl + water. Symbols represent the melting properties of ChCl obtained from Fernandez *et al.*[7] (green cross), Vilas-Boas *et al.*[31] (orange cross), Correa *et al.*[32] (yellow cross), and van den Bruinhorst *et al.*[24] (blue cross).

(see Fig. S1a in the SI, and Fig. S1b for water activity, S1c–S1e for bubble-points, S1f for freezing point depression and S1g for partial molar excess enthalpy). Thus, the calculated liquidus line of ChCl using the ion pair or dissociated ions modelling approaches can be different, as the liquidus line is influenced by ChCl activity coefficients in the liquid phase.

Fig. 8 shows the SLE phase diagram of the ChCl + water system modelled assuming ChCl as ion pairs (Fig. 8a, c and e) or fully dissociated ions (Fig. 8b, d and f) and considering the different melting properties of ChCl. As shown in Fig. 8, the influence of ChCl melting temperature on its calculated liquidus line is only noticeable at high mole fractions of ChCl. Nevertheless, at lower mole fractions of ChCl, increasing its melting temperature slightly shifts the liquidus and solidus lines to lower temperatures, in particular, as $\Delta C_{p,m}$ increases. When assuming ChCl as an ion pair (Fig. 8a, c, and e), ChCl liquidus data are better represented as $\Delta C_{p,m}$ and T_m are lower (Fig. 8a), while the eutectic point is more accurately predicted at a higher $\Delta C_{p,m}$ and T_m (Fig. 8e). In contrast, assuming ChCl as dissociated ions (Fig. 8b, d, and f) allows for representing the liquidus data at high $\Delta C_{p,m}$ and T_m (Fig. 8f). Nevertheless, the eutectic temperature is significantly underestimated when assuming ChCl as dissociated ions and considering high melting temperature and heat capacity change upon melting (Fig. 8f). This underestimation might result from extrapolating the Debye–Hückel parameter to extremely low temperatures. The Debye–Hückel parameter used in this study was adopted from Clarke and Glew,[48] which is calculated from experimental density and permittivity of water from 273.1 to 423.1 K, while the eutectic temperature of the system is close to 204 K. Neither of the modelling approaches can adequately represent liquidus data above the solid–solid transition temperature of ChCl.

Fig. 9 shows the activity coefficients of ChCl in the ChCl + water system calculated from the experimental liquidus temperature (symbols) and using the NRTL model (lines). Dashed lines represent activity coefficients of ChCl when it is regarded as ion pairs, while solid lines represent those when ChCl is considered as dissociated ions. The activity coefficients are calculated using the estimated melting enthalpy at each melting temperature together with the heat capacity change of ChCl. Because the estimated melting enthalpies when considering ChCl association or dissociation are similar (see Fig. 7), those estimated considering ChCl dissociation were used to calculate the activity coefficients from the experimental data (ΔH_m in Fig. 8b, d, and f).

As shown in Fig. 9, treating ChCl as dissociated ions (solid lines) improves the description of ChCl activity coefficients at high ChCl mole fractions, whereas assuming ChCl to be ion pairs (dashed lines) provides a better representation at low ChCl mole fractions. The calculated activity coefficients from the NRTL model assuming ChCl dissociation agree more closely with the activity coefficients derived from experimental data at T_m = 687 K and $\Delta C_{p,m}$ = 30 J mol^{-1} K^{-1} (blue crosses and solid lines in Fig. 9c). The estimated melting enthalpy (ΔH_m = 10.85 kJ mol^{-1}) at this $\Delta C_{p,m}$ and T_m is closer to that measured by van den Bruinhorst *et al.*[24] (ΔH_m = 13.8 ± 3.0 kJ mol^{-1}). On the other hand, a good description of ChCl activity coefficients could be observed when ChCl is regarded as ion pairs and T_m = 597 K and $\Delta C_{p,m}$ = 15 J mol^{-1} K^{-1} (green circles and dashed lines in Fig. 9e). The estimated melting enthalpy (ΔH_m = 7.90 kJ mol^{-1}) at this melting temperature and heat capacity change is consistent with that estimated by Vilas-Boas *et al.*[31] (ΔH_m = 7.80 kJ mol^{-1}).

As expected from the observations in Fig. 8, the activity coefficients calculated from experimental liquidus data above the solid–solid transition of ChCl cannot be described using any combination of $\Delta C_{p,m}$ and T_m in the studied range. In addition, the activity coefficients calculated from experimental data above the solid–solid transition using T_m = 687 K and $\Delta C_{p,m}$ = 30 J mol^{-1} K^{-1} seem implausible. This could be attributed to the shift in the solid–solid transition of ChCl in the presence of water. Lobo Ferreira *et al.*[25] showed that the ChCl solid–solid transition temperature shifts to around 340 K in ChCl + water, a value about 12 K lower than that of pure ChCl in the absence of water. Thus, the implausible activity coefficients calculated from the liquidus data below the solid–solid transition could in reality correspond to data above the solid–solid transition temperature.

As the melting enthalpy was estimated using experimental ChCl solubility lines data from ChCl + water and ChCl + urea simultaneously, Fig. 10 presents the SLE phase diagram of ChCl + urea calculated using the NRTL binary parameters for ChCl + urea (see Table S3). Although ChCl is always regarded as an ion pair in ChCl + urea, two different sets of binary NRTL parameters were obtained when ChCl in ChCl + water is assumed as ion pairs (Fig. 10a, c, and e) or fully dissociated ions (Fig. 10b, d, and f). The resulting binary parameters for ChCl + urea are nearly identical for both assumptions (see Table S2 in the SI), indicating that the main differences between the models when calculating the liquidus line of ChCl originate from the distinct $\Delta C_{p,m}$ and T_m used for ChCl. As previously observed for ChCl + water (Fig. 8), the melting temperature has a stronger effect on the calculated ChCl liquidus line at high mole fractions of ChCl. In particular, only a melting temperature of T_m = 597 K (yellow lines in Fig. 10) yields a satisfactory correlation of the liquidus curve near the melting point of pure ChCl. However, the influence of $\Delta C_{p,m}$ and T_m on the calculated liquidus line is less pronounced for the ChCl + urea than in the ChCl + water system (Fig. 8). In general, a better agreement between the modelled and experimental ChCl liquidus and solidus lines in ChCl + urea is observed when $\Delta C_{p,m}$ = 0 J mol^{-1} K^{-1}.

Fig. 11 shows ChCl activity coefficients calculated for the experimental liquidus data (symbols) and predicted by the NRTL model (solid lines). As before, the activity coefficients were calculated using the NRTL binary parameters and the estimated melting enthalpy when ChCl is regarded as dissociated ions in ChCl + water (see Tables S2 and S3 in the SI). Unlike the behavior observed for ChCl + water, ChCl activity coefficients in the ChCl + urea system are best reproduced when T_m = 597 K and $\Delta C_{p,m}$ = 0 J mol^{-1} K^{-1} (Fig. 11a). Neither a large $\Delta C_{p,m}$ nor a high T_m allows for accurately predicting the ChCl activity coefficients in mixtures concentrated

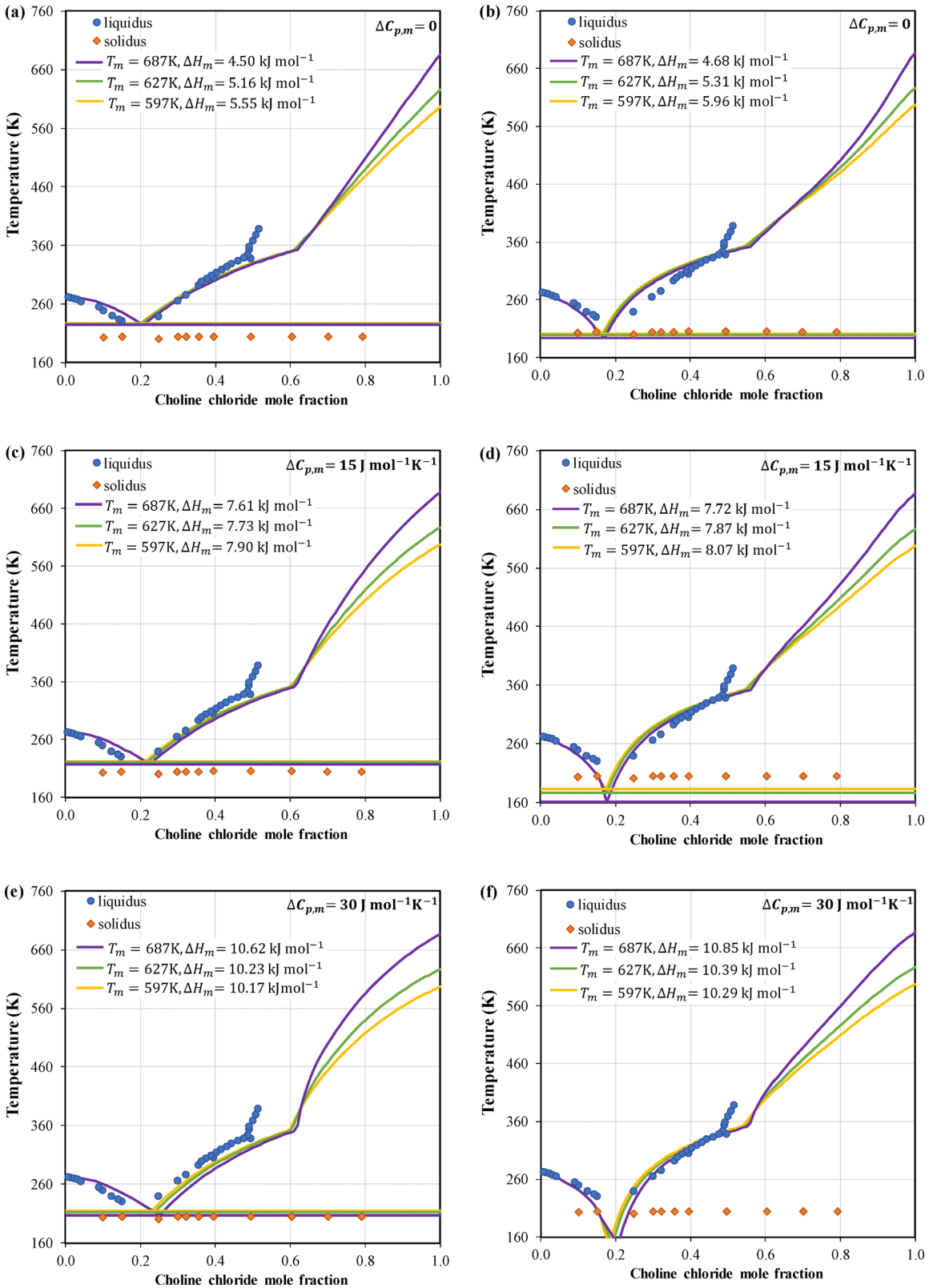

Fig. 8 Solid–liquid equilibrium phase diagram of choline chloride (ChCl) + water modeled assuming ChCl as ion pairs (a), (c), and (e) or fully dissociated ions (b), (d), and (f). The melting enthalpy (ΔH_m) used in modelling the liquidus line of ChCl was estimated in this study. Experimental data were taken from Lobo Ferreira *et al.*[25]

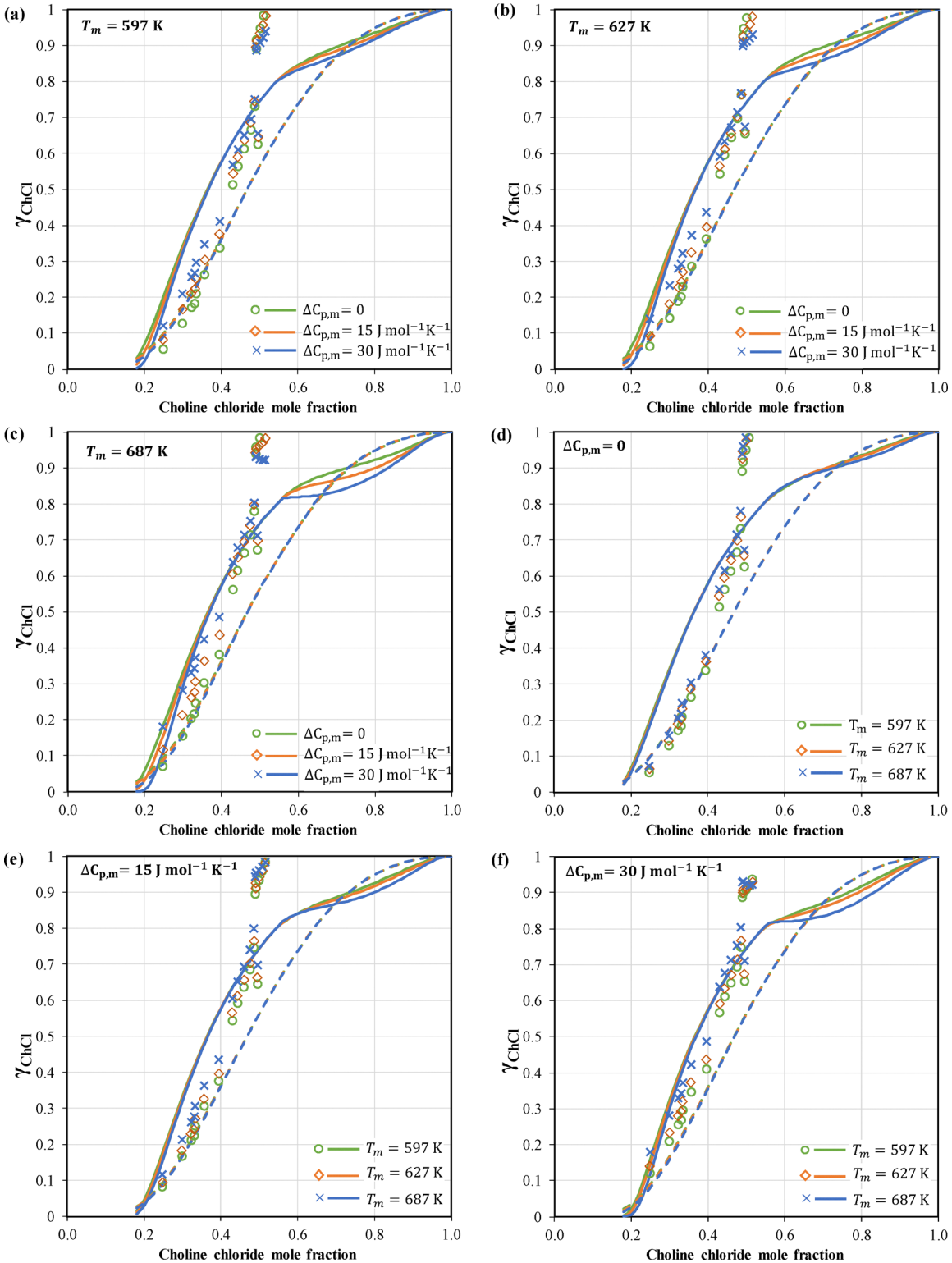

Fig. 9 Activity coefficients of choline chloride (ChCl) in ChCl + water calculated at the liquidus temperature assuming ChCl as ion pairs (dashed lines) or fully dissociated ions (solid lines). (a), (b), and (c) screening the heat capacity change at different melting temperatures, and (d), (e), and (f) screening the melting temperature at different heat capacity changes. The melting enthalpies estimated when modelling ChCl as dissociated ions were used to calculate the activity coefficients from experimental liquidus temperatures (symbols). Experimental data were taken from Lobo Ferreira *et al.*[25]

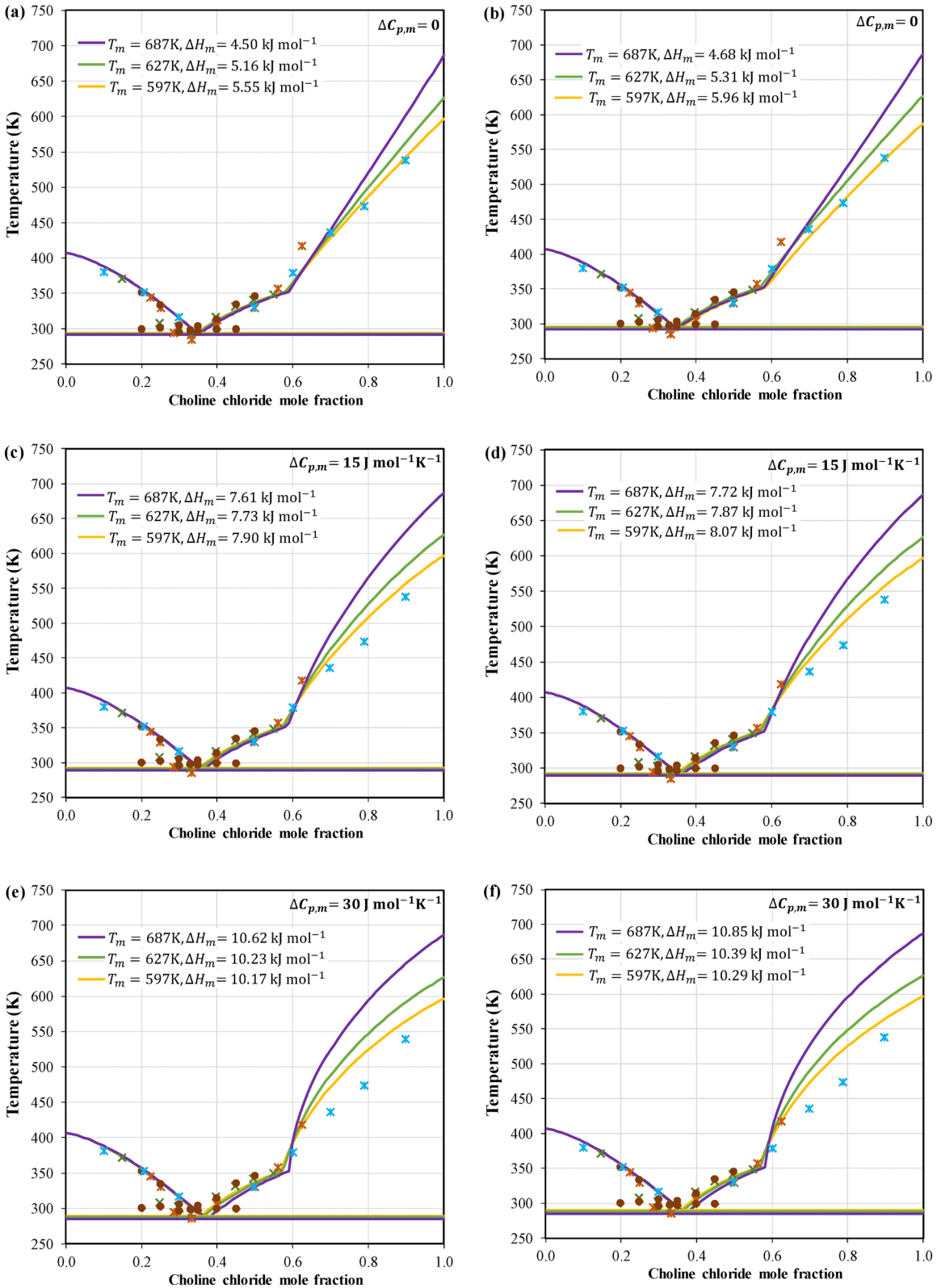

Fig. 10 Solid–liquid equilibrium phase diagram of choline chloride ChCl + urea. ChCl is always regarded as a neutral ion pair in ChCl + urea, while the ChCl + water is modeled as ion pairs (a), (c), and (e) or fully dissociated ions (b), (d), and (f). The melting enthalpy (ΔH_m) used for the modelling of the ChCl liquidus line was estimated in this study. Experimental data were taken from: × Abbot *et al.*[1] ✳ Morrison *et al.*[33] ● Meng *et al.*[34] and ✳ Silva *et al.*[35]

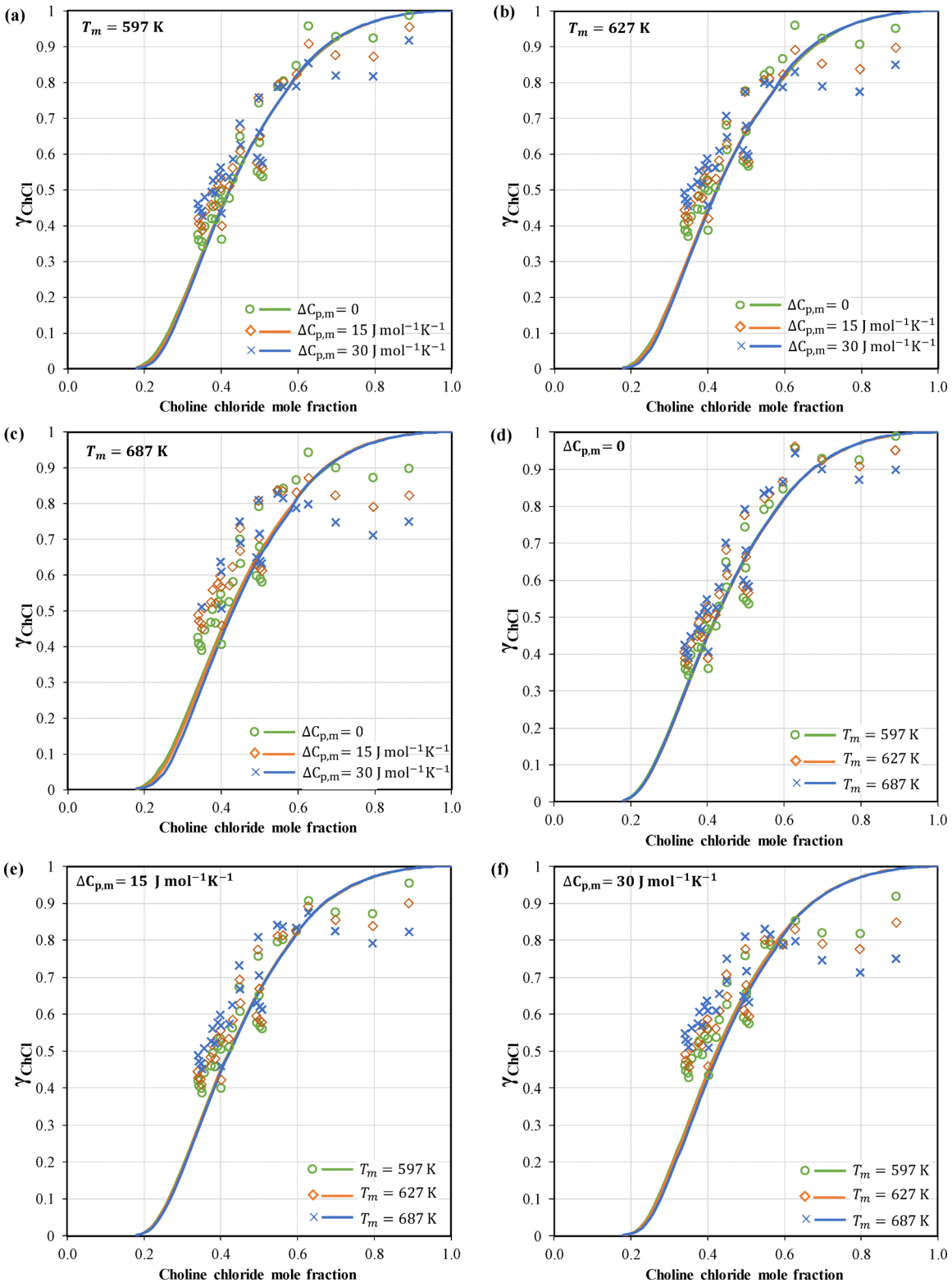

Fig. 11 Activity coefficients of choline chloride (ChCl) in ChCl + urea calculated at the liquidus temperature using the estimated melting enthalpy at each melting temperature and heat capacity change. Experimental data were taken from: Abbot *et al.*,[1] Morrison *et al.*,[33] Meng *et al.*,[34] and Silva *et al.*[35]

with ChCl (Fig. 11c and f). Moreover, the influence of the T_m is more pronounced when $\Delta C_{p,m}$ is larger. As shown in Fig. 11, the combination of T_m = 597 K and $\Delta C_{p,m}$ = 0 J mol^{-1} K^{-1} (Fig. 11a) provides the most reliable description of ChCl activity in the ChCl + urea system. The corresponding melting enthalpy (ΔH_m = 5.95 kJ mol^{-1}) is between the melting enthalpy estimated by

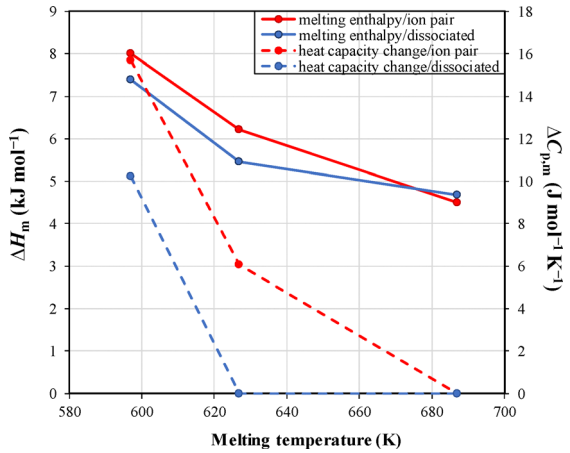

Fig. 12 The melting enthalpy (ΔH_m) and heat capacity change ($\Delta C_{p,m}$) of choline chloride (ChCl) fitted to experimental solid–liquid equilibria data of ChCl + urea and ChCl + water regarding ChCl as ion pairs or fully dissociated ions.

Fernandez *et al.*[7] (ΔH_m = 4.3 kJ mol^{-1}) and Vilas-Boas *et al.*[31] (ΔH_m = 7.80 kJ mol^{-1}).

Because the ChCl heat capacity change upon melting largely influences the estimated melting enthalpy (Fig. 7), it might be necessary to fit the $\Delta C_{p,m}$, along with its melting enthalpy and the NRTL binary parameters for ChCl + urea, to the SLE data of ChCl + urea and ChCl + water. Fig. 12 shows the melting enthalpy and heat capacity change of ChCl fitted to the SLE data of ChCl + urea and ChCl + water when assuming ChCl as ion pairs or dissociated ions in ChCl + water (see Table S5 in the SI for the data). As shown in Fig. 12, both the estimated melting enthalpy and heat capacity change decrease as the assumed melting temperature increases. When T_m = 687 K, considering $\Delta C_{p,m}$ = 0 J mol^{-1} K^{-1} is a more reasonable assumption. This behaviour is observed for ChCl + urea (Fig. 10) and not in ChCl + water (Fig. 8). The improved agreement obtained by neglecting $\Delta C_{p,m}$ can be attributed to the solubility data in ChCl + urea at higher ChCl mole fraction, where larger deviations from the experimental liquidus line occur in this region when T_m = 687 K (Fig. 11). The choice of modelling approach (ion pairs or fully dissociated ions) has little impact on the estimated melting enthalpy, but it leads to significant differences in the estimated $\Delta C_{p,m}$. The estimated melting enthalpy at T_m = 597 K is consistent with that estimated by Vilas-Boas *et al.*[31]

Conclusions

This work critically evaluates the melting properties of ChCl and demonstrates their crucial influence on the thermodynamic description of SLE in ChCl-based DES. The wide dispersion of the ChCl melting temperatures and enthalpies reported in the literature is shown to directly affect the modeling of SLE phase diagrams, calculated eutectic coordinates, and the interpretation of liquid-phase nonideality.

An essential outcome of this work is that neglecting the ChCl heat capacity change upon melting can lead to a systematic underestimation of its melting enthalpy. When the melting enthalpy is low, the heat capacity term makes a significant contribution to the calculated liquidus line of ChCl and cannot be ignored without compromising its physical consistency.

Comparative analysis of ideal and non-ideal SLE representations of ChCl + water and ChCl + urea reveals a strong interdependence between the melting properties of ChCl and its activity coefficients in the liquid phase. Low ChCl melting enthalpies artificially enforce ideal systems behaviour, while excessively high values require unrealistically strong negative deviations from ideality. Across ionic systems, including ChCl + water and ChCl + urea mixtures, melting enthalpy values between 8 and 10 kJ mol^{-1}, combined with a non-negligible heat capacity change upon melting in the range 20–40 J mol^{-1} K^{-1} (decreasing with increasing melting temperature), provide the most consistent and physically meaningful description of the experimental SLE data.

Overall, this study emphasises that the reliable melting properties of ChCl are crucial for accurately interpreting ChCl-based DES phase diagrams and for developing robust thermodynamic and data-driven models. The conclusions drawn here provide practical guidance for selecting and validating melting properties in future research.

Author contributions

Ahmad Alhadid: conceptualization, investigation, methodology, formal analysis, data curation, writing – original draft. Mirjana Minceva: conceptualization, formal analysis, resources, writing – review & editing. João A. P. Coutinho: conceptualization, formal analysis, writing – review & editing. Simão P. Pinho: conceptualization, investigation, methodology, formal analysis, data curation, writing – original draft, supervision.

Conflicts of interest

The authors declare no conflicts of interest.

Data availability

Data supporting the research findings are available in the manuscript and the supplementary information (SI). Supplementary information is available. See DOI: https://doi.org/10.1039/d6cp00187d.

Acknowledgements

This work was developed within the scope of the project CIMO-Centro de Investigação de Montanha, UIDB/00690/2020 (DOI: https://doi.org/10.54499/UIDB/00690/2020), UIDP/00690/2020 (DOI: https://doi.org/10.54499/UIDP/00690/2020); and SusTEC, LA/P/0007/2020 (DOI: https://doi.org/10.54499/LA/P/0007/2020), and CICECO-Aveiro Institute of Materials, UIDB/50011/2020 (DOI https://doi.org/10.54499/UIDB/50011/2020), UIDP/50011/

2020 (DOI https://doi.org/10.54499/UIDP/50011/2020) & LA/P/0006/2020 (DOI https://doi.org/10.54499/LA/P/0006/2020), all financed by national funds through the FCT/MCTES (PIDDAC). The financial support from IUPAC Project No. 2022-002-2-500 is highly acknowledged.

References

1 A. P. Abbott, G. Capper, D. L. Davies, R. K. Rasheed and V. Tambyrajah, *Chem. Commun.*, 2003, 70–71.
2 B. B. Hansen, S. Spittle, B. Chen, D. Poe, Y. Zhang, J. M. Klein, A. Horton, L. Adhikari, T. Zelovich, B. W. Doherty, B. Gurkan, E. J. Maginn, A. Ragauskas, M. Dadmun, T. A. Zawodzinski, G. A. Baker, M. E. Tuckerman, R. F. Savinell and J. R. Sangoro, *Chem. Rev.*, 2021, **121**, 1232–1285.
3 E. L. Smith, A. P. Abbott and K. S. Ryder, *Chem. Rev.*, 2014, **114**, 11060–11082.
4 M. A. R. Martins, S. P. Pinho and J. A. P. Coutinho, *J. Solution Chem.*, 2019, **48**, 962–982.
5 M. S. Rahman, R. Roy, B. Jadhav, M. N. Hossain, M. A. Halim and D. E. Raynie, *J. Mol. Liq.*, 2021, **321**, 114745.
6 K.-S. Kim and B. H. Park, *J. Chem. Eng. Jpn.*, 2015, **48**, 881–884.
7 L. Fernandez, L. P. Silva, M. A. R. Martins, O. Ferreira, J. Ortega, S. P. Pinho and J. A. P. Coutinho, *Fluid Phase Equilib.*, 2017, **448**, 9–14.
8 B. P. Agbodekhe, M. N. Carlozo, D. O. Abranches, K. D. Jones, A. W. Dowling and E. J. Maginn, *Mol. Syst. Des. Eng.*, 2026, **11**, 85–106.
9 M. Farshad, F. Y. M. Salih, D. O. Abranches and Y. J. Colón, *J. Chem. Phys.*, 2025, **163**, 164118.
10 A. Bazyleva, W. E. Acree, V. Diky, G. T. Hefter, J. Jacquemin, M. C. F. Magalhães, J. W. Magee, D. K. Nordstrom, J. P. O'Connell, J. D. Olson, I. Polishuk, K. A. G. Schmidt, J. M. Shaw, J. P. M. Trusler and R. D. Weir, *Pure Appl. Chem.*, 2022, **94**, 1225–1247.
11 P. Pyykkö, *ChemPhysChem*, 2019, **20**, 123–127.
12 L. J. B. M. Kollau, M. Vis, A. van den Bruinhorst, A. C. C. Esteves and R. Tuinier, *Chem. Commun.*, 2018, **54**, 13351–13354.
13 A. Alhadid, L. Mokrushina and M. Minceva, *Molecules*, 2019, **24**, 2334.
14 Z. Song, J. Wang and K. Sundmacher, *Green Energy Environ.*, 2021, **6**, 371–379.
15 D. Peng, A. Alhadid and M. Minceva, *Ind. Eng. Chem. Res.*, 2022, **61**, 13256–13264.
16 A. González de Castilla, J. P. Bittner, S. Müller, S. Jakobtorweihen and I. Smirnova, *J. Chem. Eng. Data*, 2019, **65**, 943–967.
17 Z. Song, J. Chen, H. Qin, Z. Qi and K. Sundmacher, *Chem. Eng. Sci.*, 2023, **281**, 119097.
18 P. V. d A. Pontes, E. Pereira, G. J. Maximo and E. A. C. Batista, *Fluid Phase Equilib.*, 2026, **601**, 114591.
19 K. Wang, M. Minceva and D. Peng, *Chem. Eng. Sci.*, 2026, **322**, 123130.
20 R. Wang, J. Chen, Z. Song and Z. Qi, *Ind. Eng. Chem. Res.*, 2023, **62**, 5382–5393.
21 L. B. Ayres, M. Bandara, C. D. McMillen, W. T. Pennington and C. D. Garcia, *ACS Sustainable Chem. Eng.*, 2024, **12**, 11260–11273.
22 A. K. Lavrinenko, I. Y. Chernyshov and E. A. Pidko, *ACS Sustainable Chem. Eng.*, 2023, **11**, 15492–15502.
23 F. J. López-Flores, C. Ramírez-Márquez, J. B. González-Campos and J. M. Ponce-Ortega, *Ind. Eng. Chem. Res.*, 2025, **64**, 3103–3117.
24 A. van den Bruinhorst, J. Avila, M. Rosenthal, A. Pellegrino, M. Burghammer and M. Costa Gomes, *Nat. Commun.*, 2023, **14**, 6684.
25 A. I. M. C. Lobo Ferreira, S. M. Vilas-Boas, R. M. A. Silva, M. A. R. Martins, D. O. Abranches, P. C. R. Soares-Santos, F. A. Almeida Paz, O. Ferreira, S. P. Pinho, L. M. N. B. F. Santos and J. A. P. Coutinho, *Phys. Chem. Chem. Phys.*, 2022, **24**, 14886–14897.
26 P. Shanley and R. L. Collin, *Acta Crystallogr.*, 1961, **14**, 79–80.
27 J. M. Prausnitz, R. N. Lichtenthaler and E. G. D. Azevedo, *Molecular Thermodynamics of Fluid-Phase Equilibria*, Prentice Hall PTR, Upper Saddle River, NJ, 1999.
28 J. W. Kang, V. Diky, R. D. Chirico, J. W. Magee, C. D. Muzny, A. F. Kazakov, K. Kroenlein and M. Frenkel, *J. Chem. Eng. Data*, 2014, **59**, 2283–2293.
29 L. P. Cunico, R. Ceriani, B. Sarup, J. P. O'Connell and R. Gani, *Fluid Phase Equilib.*, 2014, **362**, 318–327.
30 V. Petrouleas and R. M. Lemmon, *J. Chem. Phys.*, 1978, **69**, 1315–1316.
31 S. M. Vilas-Boas, D. O. Abranches, E. A. Crespo, O. Ferreira, J. A. P. Coutinho and S. P. Pinho, *J. Mol. Liq.*, 2020, **300**, 112281.
32 G. B. Correa, D. O. Abranches, E. Marin-Rimoldi, Y. Zhang, E. J. Maginn and F. W. Tavares, *J. Phys. Chem. Lett.*, 2024, **15**, 11801–11805.
33 H. G. Morrison, C. C. Sun and S. Neervannan, *Int. J. Pharm.*, 2009, **378**, 136–139.
34 X. Meng, K. Ballerat-Busserolles, P. Husson and J.-M. Andanson, *New J. Chem.*, 2016, **40**, 4492–4499.
35 L. P. Silva, C. F. Araújo, D. O. Abranches, M. Melle-Franco, M. A. R. Martins, M. M. Nolasco, P. J. A. Ribeiro-Claro, S. P. Pinho and J. A. P. Coutinho, *Phys. Chem. Chem. Phys.*, 2019, **21**, 18278–18289.
36 H. Marques, A. González de Castilla, S. Müller and I. Smirnova, *Fluid Phase Equilib.*, 2023, **569**, 113765.
37 M. Francisco, A. S. B. González, S. L. García de Dios, W. Weggemans and M. C. Kroon, *RSC Adv.*, 2013, **3**, 23553–23561.
38 S. Gholami and A. Roosta, *J. Mol. Liq.*, 2019, **296**, 111876.
39 P. J. Carvalho, I. Khan, A. Morais, J. F. O. Granjo, N. M. C. Oliveira, L. M. N. B. F. Santos and J. A. P. Coutinho, *Fluid Phase Equilib.*, 2013, **354**, 156–165.

40 I. Khan, K. A. Kurnia, T. E. Sintra, J. A. Saraiva, S. P. Pinho and J. A. P. Coutinho, *Fluid Phase Equilib.*, 2014, **361**, 16–22.
41 P. Velho, E. Sousa and E. A. Macedo, *Fluid Phase Equilib.*, 2025, **587**, 114197.
42 A. van den Bruinhorst, C. Corsini, G. Depraetère, N. Cam, A. Pádua and M. Costa Gomes, *Faraday Discuss.*, 2024, **253**, 273–288.
43 R. Fleming, *J. Chem. Soc.*, 1961, 3100–3102.
44 J. B. Macaskill, M. S. Mohan and R. G. Bates, *Anal. Chem.*, 1977, **49**, 209–212.
45 G. E. Boyd, A. Schwarz and S. Lindenbaum, *J. Phys. Chem.*, 1966, **70**, 821–825.
46 F. I. Travaglini, L. Romagnoli, A. M. Czerska, M. Busato, G. Mannucci, S. Vecchio Ciprioti, P. D'Angelo and A. Ciccioli, *Phys. Chem. Chem. Phys.*, 2025, **27**, 25266–25270.
47 J. Timmermans, *J. Phys. Chem. Solids*, 1961, **18**, 1–8.
48 E. C. W. Clarke and D. N. Glew, *J. Chem. Soc., Faraday Trans. 1*, 1980, **76**, 1911–1916.